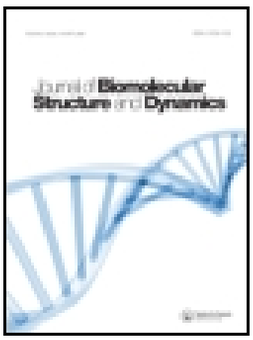

Taylor & Francis
Taylor & Francis Group

Journal of Biomolecular Structure and Dynamics

ISSN: (Print) (Online) Journal homepage: https://www.tandfonline.com/loi/tbsd20

Synthesis, antioxidant, *in silico* and computational investigation of 2,5-dihydroxyacetophenone derived chloro-substituted hydroxychalcones, hydroxyflavanones and hydroxyflavindogenides

Aysha Siddiqa, Affifa Tajammal, Ahmad Irfan, Munawar Ali Munawar, Muhammad Azam & Muhammad Asim Raza Basra

To cite this article: Aysha Siddiqa, Affifa Tajammal, Ahmad Irfan, Munawar Ali Munawar, Muhammad Azam & Muhammad Asim Raza Basra (2021): Synthesis, antioxidant, *in silico* and computational investigation of 2,5-dihydroxyacetophenone derived chloro-substituted hydroxychalcones, hydroxyflavanones and hydroxyflavindogenides, Journal of Biomolecular Structure and Dynamics, DOI: 10.1080/07391102.2021.1943527

To link to this article: https://doi.org/10.1080/07391102.2021.1943527

JOURNAL OF BIOMOLECULAR STRUCTURE AND DYNAMICS
https://doi.org/10.1080/07391102.2021.1943527

Synthesis, antioxidant, *in silico* and computational investigation of 2,5-dihydroxyacetophenone derived chloro-substituted hydroxychalcones, hydroxyflavanones and hydroxyflavindogenides

Aysha Siddiqa[a], Affifa Tajammal[a,b], Ahmad Irfan[c,d], Munawar Ali Munawar[a], Muhammad Azam[a] and Muhammad Asim Raza Basra[a]

[a]School of Chemistry, University of the Punjab, New Campus, Lahore, Pakistan; [b]Department of Chemistry, Lahore Garrison University, Lahore, Pakistan; [c]Department of Chemistry, Faculty of Science, King Khalid University, Abha, Saudi Arabia; [d]Research Center for Advanced Materials Science (RCAMS), King Khalid University, Abha, Saudi Arabia

Communicated by Ramaswamy H. Sarma.

ABSTRACT

An imbalance between reactive oxygen species (ROS) and their elimination by antioxidants damages the cell and infect whole organism. The biological defence system against oxidative stress injury is Kelch-like ECH associated protein 1 (Keap1)-nuclear factor erythroid 2-related factor 2 (Nrf2)-antioxidant response elements (ARE) pathways. Antioxidants activate the Nrf2-ARE-Keap1 pathway and suppress the oxidative stress. Flavonoids are well known medicinal compounds inheriting antioxidant efficacy and wide spectrum of pharmacological activities. The study is aimed to synthesise, characterize and evaluate pharmacological activities of synthesized chloro-derivatives of flavonoids. Chloro-derivatives of flavonoids were synthesized and characterized by IR, ^{1}H NMR and ^{13}C NMR. Antioxidant potential of each synthesized compound was evaluated and then subjected to molecular docking with Keap1 (PDB ID: 2FLU) for the activation of Nrf2 and computational studies were performed by using DFT approach. Among the synthesized compounds compound 1a exhibited lower IC_{50} value. While docking and computational studies infer that compound 3c is a good Nrf2 activator and radical scavenger with highest docking score and lower energy gaps and IP values compared to references. Hence, it might be considered for further molecular studies for the treatment of inflammatory diseases through Nrf2-ARE-Keap1 pathway.

HIGHLIGHTS

- Chloro-substituted hydroxychalcones, hydroxyflavanones and hydroxyflavindogenides were synthesized.
- Antioxidant potential was accessed, compound 1a exhibited good antioxidant potential.
- *In silico* study was performed with Keap1, compound 3c have shown highest docking score with Keap1.
- DFT approach was used to explore the structure activity relationship.

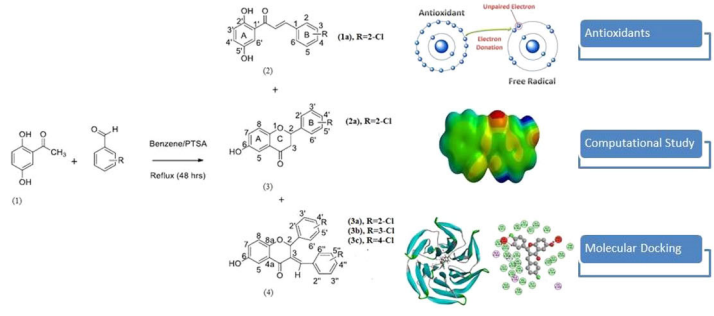

Abbreviations: ABTS: 2,2′-Azino-bis(3-ethylbenzothiazoline-6-sulphonic acid); ACE: Atomic Contact Energy; Ar: Aromatic; ARE: Antioxidant response elements; ATP: Adenosine diphosphate; d: Doublet; *d*: Deutrated; dd: Doublet of doublet; DFT: Density Functional Theory; DMSO: Dimethylsulfoxide; DPPH: 2,2-diphenyl-1-picrylhydrazyl; DNA: Deoxyribonucleic acid; DS: Discovery Studio; E_{gap}: Energy gaps; FLS: Fibroblast-like synoviocytes; FMOs: Frontier molecular orbitals; FT-IR: Fourier-transform infrared spectroscopy; g: Gram; HO-1: Heme oxygenase-1; HOMOs: Highest occupied molecular orbitals; *hv*:

ARTICLE HISTORY
Received 14 March 2021
Accepted 3 June 2021

KEYWORDS
Flavonoids; antioxidants; computational; Nrf2; molecular docking

CONTACT Muhammad Asim Raza Basra asimbasra.chem@pu.edu.pk School of chemistry, University of The Punjab, New Campus, Lahore, Pakistan
Supplemental data for this article can be accessed online at https://doi.org/10.1080/07391102.2021.1943527.

SunlightHzHertz; IC_{50}: Half maximal inhibitory concentration; ICT: Intra-molecular charge transfer; IP: Ionization potentials; IR: Infrared; *J*: Coupling constant; Keap1: Kelch-like ECH associated protein 1; LUMOs: Lowest unoccupied molecular orbitals; MEP: Molecular electrostatic potential; mL: Millilitre; mM: Millimole; M: Mole; MS: Mass Spectroscopy; Nm: Nanometer; NMR: Nuclear Magnetic Resonance; Nrf2: Nuclear factor erythroid 2-related factor 2; PDB: Protein Data Bank; QSAR: Quantitative structure-activity relationship; RASFs: Synovial fibroblasts derived from RA patients; RCSB: Research Collaboratory for Structural Bioinformatics; ROS: Reactive oxygen species; SAR: Structure-activity relationship; TLC: Thin layer chromatography

Introduction

Flavonoids are one of the largest classes of polyphenolic compounds widely distributed in plants, possessing extensive antioxidant, medicinal and chelating properties (Heim et al., 2002). Structurally flavonoids have a skeleton of 15-carbons, consisting of two benzene rings (A and B rings) joined via a 3-carbon chain that forms a heterocyclic pyran ring (C) (Figure 1) (Amic et al., 2007). They could be further classified into major groups depending on their chemical structure, degree of oxidation and linking chain un-saturation flavonoids i.e. flavonols, dihydroflavonols, chalcones, isoflavones, dihydroisoflavones, bioflavonoids, orange ketones and anthocyanidins (Atwood & Buck, 2020). Flavonoids have been reported beneficial for human health and exhibit a wide range of pharmacological activities such as antioxidant, antidiabetic, anti-inflammatory, antibacterial, anticancer and antiviral activities, vasodilating actions and hepatoprotective effect (Abotaleb et al., 2018; Ashraf et al., 2020; Górniak et al., 2019; Karak, 2019; Maleki et al., 2019; Pietta, 2000). Though, antioxidant activities of flavonoids has gained uppermost interest due to their ability to scavenge and reduce free radical formation (Pietta, 2000).

Free radicals are reactive oxygen species (ROS) produced continuously in all cells as part of normal cellular function and various environmental factors (Young & Woodside, 2001). However, excessive production of ROS leads to oxidative stress consequently miscellaneous damage to cells comprising upswing of cytosolic Ca^{2+}, decline of ATP level in cells, DNA damage, and biological dysfunction in lipid bilayer. These deleterious effects result in all kind of diseases (Mao et al., 2017). Antioxidants are the substances which reduce oxidative stress and modulate its consequences by combating ROS (Halliwell et al., 1995).

Various researchers have explored the antioxidant activity of flavonoids and numerous efforts have been made to investigate the structure activity relationship (SAR). It has been established that antioxidant activity of flavonoids is dependent on structure (Sarian et al., 2017). Mughal et al. synthesized derivatives of 3-benzyloxyflavone and determined their cholinesterase inhibitory potential including acetylcholinesterase (0.05) and butyrylcholinesterase (0.09) (Mughal et al., 2020). Ashraf et al. synthesized flavonols and studied their dual inhibitory effect for α-amylase and α-glucosidase along with SAR via *in vitro and in silico* studies (Ashraf et al., 2020). Ashraf et al. also designed and synthesized 2-phenylchromone derivatives as potent tyrosinase inhibitors via *in vitro* and *in silico* studies (Ashraf et al., 2021). Yang et al. reported 90.4% DPPH radical scavenging activity of rutin at the concentration of 0.05 mg/mL (Yang et al., 2008). Singh et al. determined the antioxidant potential of common flavonoids via DPPH, ABTS and deoxyribose protection assay. They reported catechin hydrate, the strongest antioxidant compound (IC_{50}; 8.34, 4.93 and 5.96 µg/mL) among 3-hydroxyflavone (IC_{50}; 503.7, 20.83, 216.5 4), 7-hydroxyflavone (IC_{50} ND, 19.35, 96.4), t-chalcone (IC_{50} ND 225.7, 542.8), hesperetin (IC_{50}; 363.7, 8.37, 97.1), flavanone (IC_{50}; 2707.8, 525.8, 99.68), quercetin (IC_{50}; 6.55, 13.78, 7.58), rutin (IC_{50}; 9.44, 14.6 3, 1.2 9.87), quercetin hydrate (IC_{50}; 4.71, 10.6 3, 20.1) and kaempferol (IC_{50}; 17.30, 8.54, 7.17) (Singh et al., 2018) (Figure 2).

Nuclear factor erythroid 2-related factor 2 (Nrf2), a transcriptional factor, is found to play a central role in moderating cellular protection against oxidative stress as well as ameliorate the inflammatory response (Tran et al., 2018; Zhang et al., 2019). Kelch-like ECH-associated protein 1 (Keap1) is an inhibitor of Nrf2. Under normal conditions, Keap1 forms a complex with Nrf2 leading to its proteasomal degradation and inactivation (Sun et al., 2017). Upon exposure to oxidative stress, Nrf2 detaches from Keap1 and translocates into the nucleus where it binds to antioxidant response elements (ARE) and induces the expression of a battery of endogenous antioxidant, cytoprotective enzymes to provide cellular protection (Bresciani et al., 2017). Targeting Nrf2 signalling has emerged as a core and effective therapy to treat or lower the risk of diseases caused by oxidative stress (Zhai et al., 2018).

Flavonoids are among the most noticeable phytochemicals that suppress inflammation by triggering Nrf2 pathway (Li et al., 2019). Many natural flavonoids has been pinpointed as therapeutic agents for human diseases through Nrf2 activation, some commercially available flavonoids are taxifolin, quercetin, procyanidins genistein and kaempferol (Li et al., 2018). Calycosin suppresses the expression of pro-inflammatory cytokines by inducing p62/Nrf2-linked HO-1 pathway in synovial fibroblasts derived from RA patients (RASFs) (Su et al., 2016). Wu et al. also reported that dihydromyricetin inhibits the expressions of pro-inflammatory cytokines in RA model via activating Nrf2 pathway (Wu et al., 2016). Resveratrol attenuated RA through activation of Nrf2-ARE signaling pathway via SIRT1/NF-κB/miR-29a-3p/Keap1 and SIRT1/NF-κB/miR-23a-3p/cul3 signaling pathway in primary rat fibroblast-like synoviocytes (FLS) (Wang et al., 2020).

Owing to the diverse biological activities of flavonoids, new flavonoid derivatives were synthesized and characterized. Moreover, the synthesized compounds were explored for their *in vitro* and *in silico* antioxidant activities. Molecular docking of all synthesized compounds was performed to find

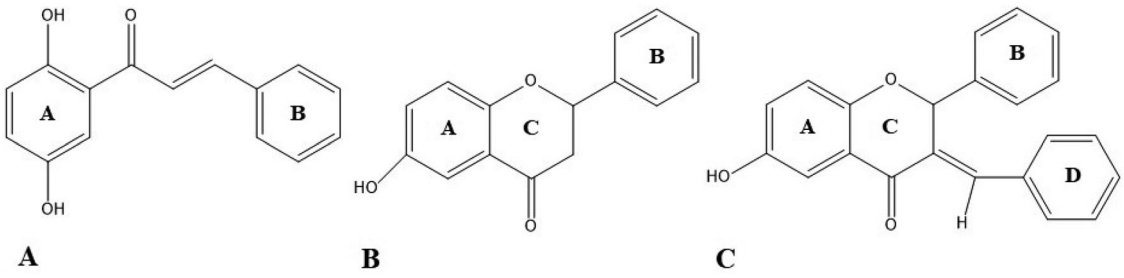

Figure 1. **Structures of flavonoids.** Hydroxychalcones (A), hydroxyflavanones (B) and hydroxyflavindogenides (C).

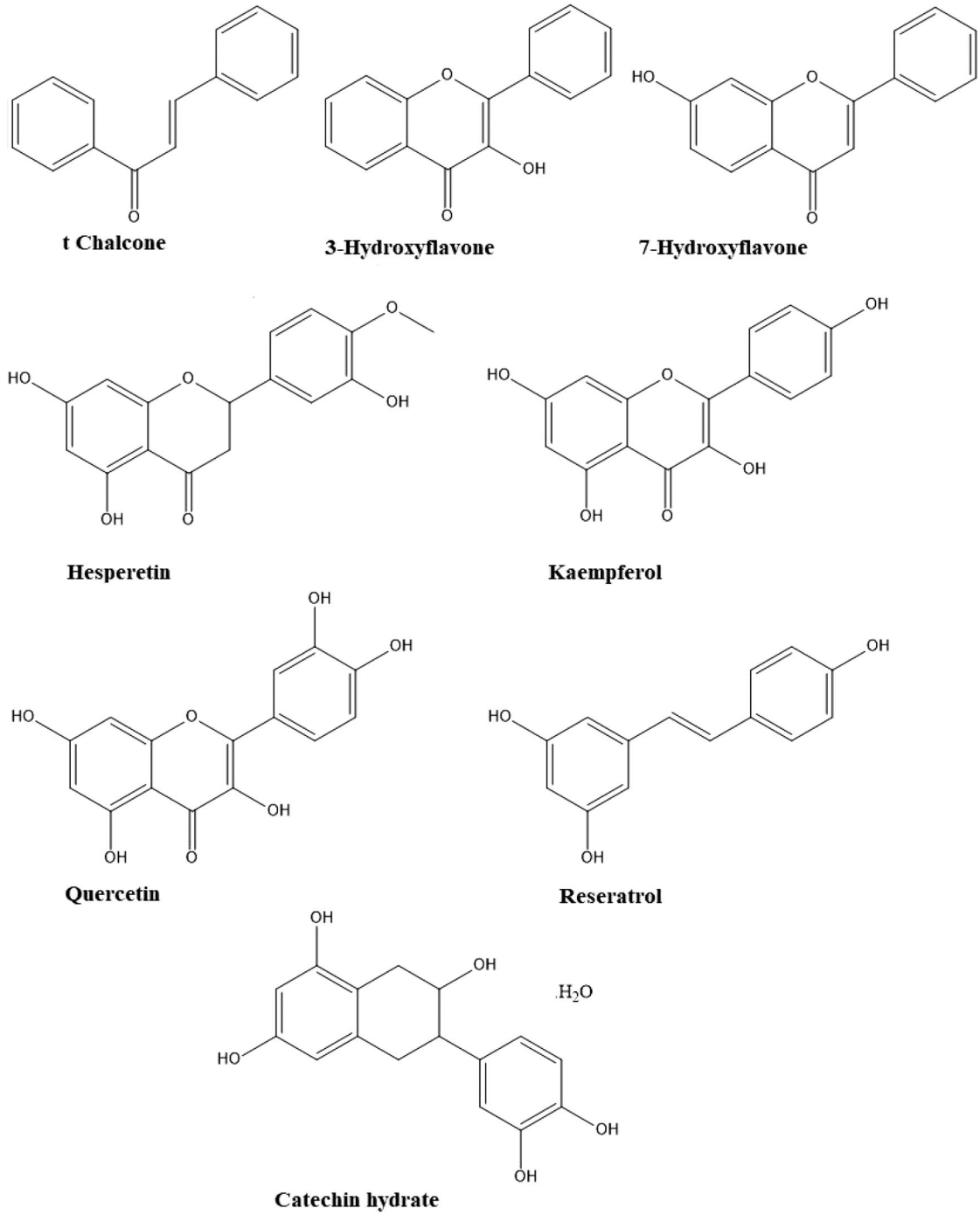

Figure 2. Structures of some potent flavonoids.

their affinity for Keap1 and activation of Nrf2. DFT was used to study the radical scavenging activity of the synthesized compounds by hydrogen atom transfer and one electron transfer mechanisms.

Experimental

Materials and methods

Previously reported method was used to synthesize the 2,5-dihydroxyacetophenone (Amin & Shah, 2003). Silica gel 60 F254 TLC plates were used to observe the reaction while FT-IR, ^{1}H NMR and ^{13}C NMR spectra and EIMS data were recorded on Agilent Technologies 41630, AVANCE AV-400 MHz and AVANCE AV-500 MHz, Bruker 125 MHz and JEOL MS 600H-1respectively.

General method for the synthesis of flavonoids

First, 0.3 mM 2,5-dihydroxyacetophenone (Sigma-Aldrich), 0.3 mM chlorobenzaldehyde (Sigma-Aldrich) and 20 mL benzene (Sigma-Aldrich) were mixed. This resulting mixture was added in 0.03 mM *p*-toluene sulfonic acid (Parchem) and refluxed it for 48 h. Thin layer chromatography (TLC) (Merck) was used to observe the reaction status at different time. After the completion of reaction, benzene was evaporated completely under vacuum. Finally the residue was purified by using ethyl acetate:hexanes (4:1) (Commercial) as eluent in silica gel column to obtain compounds 1a, 2a, 3a, 3b and 3c.

(E)-3-(2-Chlorophenyl)-1-(2,5-dihydroxyphenyl)prop-2-en-1-one (1a)

Physical state: solid; appearance: orange powder; yield: 0.3 g (18 %); melting point: 213 °C; Rf value: 0.6 (ethyl acetate: hexanes 1:4); FT-IR: υ (cm^{-1}): 3358 (-OH), 3060 (Ar-H), 1686 (C = O), 1577, 1507 (C = C), 760 (C-Cl). ^{1}H NMR: (500 MHz/DMSO-*d6*): δ 11.46 (1H, s, 2′-OH), 9.19 (1H, s, 5′-OH), 8.17 (1H, d, J = 7.3 Hz, 6-H), 8.07 (1H, d, J = 15.5 Hz, β-H), 7.96 (1H, d, J = 15.5 Hz, α-H), 7.59 (1H, d, J = 7.6 Hz, 3-H), 7.52-7.45 (3H, m,4- H, 5-H, 6′-H), 7.06 (1H, dd, J = 8.8, 2.8 Hz, 4′-H), 6.87 (1H, d, J = 8.8 Hz, 3′-H). 13 C NMR: δ 193.13 (C = O), 154.76 (2′-C), 150.09 (5′-C), 138.91 (β-C), 134.89 (1- C), 132.65 (2-C), 132.63 (3-C), 130.56 (4-C), 129.18 (6-C), 128.26 (5- C), 125.97 (1′-C), 124.95 (α-C), 121.79 (4′-C), 118.84 (3′-C), 115.64 (6′-C).

2-(3-Chlorophenyl)-6-hydroxychroman-4-one (2a)

Physical state: solid; appearance: light orange powder; yield: 0.2 g (12 %); melting point: 202 °C; Rf value: 0.8 (ethyl acetate: hexanes 1:4); FT-IR: υ (cm^{-1}): 3351 (-OH), 3054 (Ar-H), 1654 (C = O), 1578, 1521 (C = C), 754 (C-Cl). 1H NMR: (500 MHz/DMSO-*d6*): δ 9.48 (1H, s, 6-OH), 7.78 (1H, d, J = 7.35 Hz 3′-H), 7.61-7.53 (1H, m, 4′-H), 7.49-7.44 (2H, m, 5′-H, 6′-H), 7.13 (1H, d, J = 1.8 Hz, 5-H), 7.06 (1H, dd, J = 8.8, 2.9 Hz, 7-H), 6.98 (1H, d, J = 8.8 Hz, 8-H), 5.79 (1H, dd, J = 13.3, 1.65 Hz, 2-H), 3.19 (1H, dd, J = 16.6, 13.8 Hz, Ha), 2.79 (1H, dd, J = 16.8, 2.3 Hz, Hb). 13 C NMR: δ 191.71 (C = O), 154.77 (8a-C), 152.33 (6-C), 152.28 (3′-C), 137.51 (1′- C), 131.94 (2′-C), 130.69 (3′-C), 128.61 (4′-C), 128.18 (6′-C), 125.09 (5′-C), 121.26 (5-C), 120.65 (7-C), 119.43 (4a-C), 110.52 (8-C), 76.29 (2-C), 42.84 (3-C).

(E)-3-(2-Chlorobenzylidene)-2-(2-chlorophenyl)-6-hydroxychroman-4-one (3a)

Physical state: solid; appearance: yellow needles; yield: 0.4 g (17 %); melting point: 276 °C; Rf value: 0.72 (ethyl acetate: hexanes 1:4); FT-IR: υ (cm^{-1}) 3358 (-OH), 3060 (Ar-H), 1654 (C = O), 1575, 1456 (C = C), 1214 (C-O), 764 (C-Cl). 1H NMR: (500 MHz/DMSO-*d6*): δ 9.64 (1H, s, 6-OH), 8.01 (1H, s, C = C-H), 7.58 (1H, d, J = 8.0 Hz, 6′′-H), 7.55 (1H, d, J = 8.0 Hz, 3′-H), 7.44 (1H, t, J = 8.0 Hz, 4′′-H), 7.38 (1H, dt, J = 8.0,1.4 Hz, 4′-H), 7.31-7.25 (2H, m, 5′- H, 5′′-H), 7.23 (1H, d, J = 3.0 Hz, 5-H), 7.13 (1H, d, J = 8.9 Hz, 3′′-H), 7.98 (1H, dd, J = 3.0, 8.3 Hz, 7-H), 6.78 (1H, d, J = 7.6 Hz, 8-H), 6.73 (1H, d, J = 8.8 Hz, 6′-H), 6.55 (1H, s, 2-H). 13 C NMR: (125 MHz/DMSO-*d6*): δ181.45 (C = O), 152.80 (8a-C), 151.64 (6-C),136.06 (1′-C), 135.86 (=CH), 134.27 (2′′-C), 133.99 (3-C), 133.92 (1′′-C), 132.15 (3′′-C), 132.02 (4′′-C), 131.65 (3′-C), 131.08 (4′-C), 130.47 (5′-C), 129.87 (6′-C), 129.75 (6′′-C), 127.92 (5′′-C), 127.82 (2′-C), 125.99 (7-C), 121.97 (4a-C), 120.13 (8-C), 111.07(5-C), 75.36 (2-C).MS (EI+): *m/z* 396 (M+, 1.4%), 361 (100), 326 (1.7), 297 (1.7), 278 (2.0), 251 (1.6), 225 (10), 189 (8.5), 163 (2.5), 136 (7.3).

(E)-3-(3-Chlorobenzylidene)-2-(3-chlorophenyl)-6-hydroxychroman-4-one (3b)

Physical state: solid; appearance: yellow needles; yield: 0.8 g (34 %); melting point: 289 °C; Rf value: 0.9 (ethyl acetate: hexanes 1:4); FT-IR: υ (cm^{-1}): 3375 (-OH), 3078 (Ar-H), 1670 (C = O), 1577, 1458 (C = C), 681 (C-Cl). 1H NMR: (500 MHz/DMSO-*d6*): δ 9.59 (1H, s, 6-OH), 7.99 (1H, s, C = C-H), 7.53-7.41 (6H, m, 2′-H, 4′-H, 2′′-H, 6′′-H, 4′′-H, 5′′-H), 7.30-7.25 (2H, m, 5′- H, 6′-H), 7.11 (1H, d, J = 3.0 Hz, 5-H), 7.01 (1H, dd, J = 3.0, 8.8 Hz, 7- H), 6.94 (1H, d, J = 8.8 Hz, 8-H), 6.63 (1H, s, 2-H). 13 C NMR: (125 MHz/DMSO-*d6*): δ 181.53 (C = O), 152.73 (8a-C), 151.76 (6-C), 140.75 (1′-C), 138.31 (=CH), 135.82 (1′′-C), 134.27 (3′-C), 134.16 (3′′- C), 133.13 (3-C), 131.39 (5′-C, 5′′-C), 130.29 (2′′-C), 130.21 (4′′-C), 129.36 (4′-C), 128.47 (6′′-C), 127.51 (2′-C), 126.38 (6′-C), 125.77 (7- C), 122.18 (4a-C), 120.43 (8-C), 111.00(5-C), 89.76 (2-C). MS (EI+): *m/z* 396 (M+, 72%), 361 (13.2), 297 (1.7), 285 (19.2), 260 (16.6), 225 (28.3), 189 (23.7), 163 (1.9), 137 (100), 136 (85.5).

(E)-3-(4-Chlorobenzylidene)-2-(4-chlorophenyl)-6-hydroxychroman-4-one (3c)

Physical state: solid; appearance: yellow needles; yield: 0.95 g (38 %); melting point: 292 °C; Rf value: 0.8 (ethyl acetate: hexanes 1:4); FT-IR: υ (cm^{-1}): 3388 (-OH), 3051 (=C-H), 1665 (C = O), 1598, 1492 (C = C), 768 (C-Cl). 1H NMR: (500 MHz/DMSO-*d6*): δ9.48 (1H, s, 6-OH), 7.99 (1H, s, C = C-H), 7.53 (2H, d, J = 8.3 Hz, 2′′-H, 6′′-H), 7.45 (2H, d, J = 8.4 Hz, 5′-H, 6′-H), 7.40–7.38 (4H, m,3′-H, 5′-H, 3′′-H, 5′′-H), 7.11 (1H, d, J = 2.6 Hz, 5-H), 6.99 (1H, dd, J = 2.8, 8.8 Hz, 7-H), 6.91 (1H, d, J = 8.8 Hz, 8-H), 6.62 (1H, s, 2-H). 13 C NMR: (125 MHz/DMSO-*d6*): δ181.64 (C = O), 152.71 (8a-C), 151.68 (6-C), 138.25 (=CH), 137.26 (1′-C), 135.36 (4′′-C), 133.96 (3-C), 132.74 (4′-C), 132.66 (1′′-C), 132.22 (2′′-C, 6′′-C), 129.66 (3′-C, 5′-C), 129.61 (3′′- C, 5′′-C), 129.47 (2′-C, 6′-C), 125.52 (7-C), 122.30 (4a-C), 120.36 (8- C), 111.06 (5-C), 76.48 (2-C). MS (EI+): *m/z* 396

(M+, 78%), 361 (18), 297 (2), 285 (12), 260 (14), 225 (67), 189 (37), 163 (8), 137 (100), 136 (87).

In vitro antioxidant activities

DPPH free radical scavenging activity

Free radical scavenging activity of synthesized compounds was evaluated by DPPH assay. 0.15 mL of different concentrations of test compounds was mixed with 2.85 mL of ethanolic DPPH (0.05 mM) (Sigma-Aldrich) solution and incubated in dark at 37 °C. The absorbance was recorded at 517 nm after 15, 30, 45, 60 and 120 mins of incubation (Tajammal et al., 2017). The percentage activity was calculated with following equation:

$$\%\text{Scavengingactivity} = (A_c - A_t/A_c) \times 100$$

where, A_c = absorbance of control and A_t = absorbance of test compound.

ABTS activity

2,2′-Azino-bis-3-ethylbenzothiazoline-6-sulfonic acid (ABTS) regent (bio WORLD) was used to estimate $ABTS^+$ scavenging activity. Aqueous solution of ABTS (7 mM) was mixed with 2.4 mM aqueous potassium persulfate (Sigma-Aldrich) solution and left in dark for about 16 h at room temperature. For antioxidant assay, the solution was diluted with ethanol (Merk) to set absorbance to 0.7 ± 0.02 at 734 nm. Finally, 0.15 mL of various concentrations of test compounds in ethanol was mixed with ABTS reagent. The absorbance was recorded after 5, 15, 30, 45, 60 and 120 mins of incubation at 734 nm. Following relation was used to calculate the % scavenging activity (Tajammal et al., 2017).

$$\%\text{scavengingactivity} = (A_c - A_t/A_c) \times 100$$

where, A_c = absorbance of control and A_t = absorbance of test compound.

Iron chelating activity

Iron chelation was determined by adding 0.05 % methanolic o-phenanthroline (ACROS ORGANICS) and 200 mM methanolic ferric chloride (ICON CHEMICAL) solutions in different concentrations of the test compounds. The mixture was incubated at room temperature and absorbance was measured after 10, 30, 45, 60 and 120 mins at 512 nm. % activity was determined by using the following formula (Tajammal et al., 2017).

$$\%\text{reducingpower} = (A_t/A_c - 1) \times 100$$

where, A_c =absorbance of control and A_t = absorbance of test compound.

$FeCl_3$ reducing power activity

$FeCl_3$ reducing power was measured by adding 1 % potassium ferricyanide (ACROS ORGANICS) to different dilutions of tested compounds. The resulting mixture was incubated for 20 mins at 50 °C and cooled to room temperature. Then 10 % trichloroacetic acid (AnalaR NORMAPUR) was added to the resulting mixture and centrifuged for 10 mins at 3000 rpm. Supernatant was diluted with equal volume of distilled water and mixed with 1 mL of freshly prepared 0.1 % aqueous solution of ferric chloride. The reaction mixture was incubated at room temperature and absorbance was recorded after 10, 30, 45, 60 and 120 mins at 700 nm. % reducing power was calculated by the following equation (Tajammal et al., 2017).

$$\%\text{reducingpower} = (A_t/A_c - 1) \times 100$$

where, A_c = absorbance of control and A_t = absorbance of test compound.

Phosphomolybdenum activity

Phosphomolybdenum (PM) activity was measured by using PM reagent (0.6 M sulphuric acid + 28 mM sodium phosphate + 4 mM ammonium molybdate). Different concentrations of tested compounds were prepared and PM reagent was added to each concentration. The reaction mixture was incubated for 1:30 h at 95 °C and absorbance was recorded after 15, 30 and 45 mins at 765 nm. % reducing power was calculated by using the following equation (Tajammal et al., 2017).

$$\%\text{reducingpower} = (A_t/A_c - 1) \times 100$$

where, A_c = absorbance of control and A_t = absorbance of test compound.

In silico evaluations

Molecular docking of the synthesized flavonoids was carried out against Keap1. Three-dimensional crystal structure of the Keap1 protein was obtained from the Research Collaboratory for Structural Bioinformatics (RCSB) Protein Data Bank (PDB ID: 2FLU at 1.50 Å resolution) (Athar et al., 2016).

Preparation of target Keap 1 and compounds for docking

Discovery Studio (DS) 4.5 Visualizer was used to prepare receptor protein for docking by removing water molecules and adding hydrogen atoms. Three-dimensional structures of the synthesized compounds were drawn and optimized by using Avogadro software. All the files of receptor protein and compounds were saved in PDB format (Athar et al., 2016).

Binding pockets determination

Protein binding pocket was visualized by using Deepsite-PlayMolecule and the amino acids surrounding the binding pocket were noted (Jiménez et al., 2017).

Receptor-ligand interaction

Docking of the synthesized compounds individually against Keap1 was performed by using Patch Dock which works on the shape complementarity principles (Schneidman-Duhovny et al., 2005). The docking results were selected in view of the amino acid residues in the binding pocket. The receptor-ligand interaction was evaluated on the basis of docking score

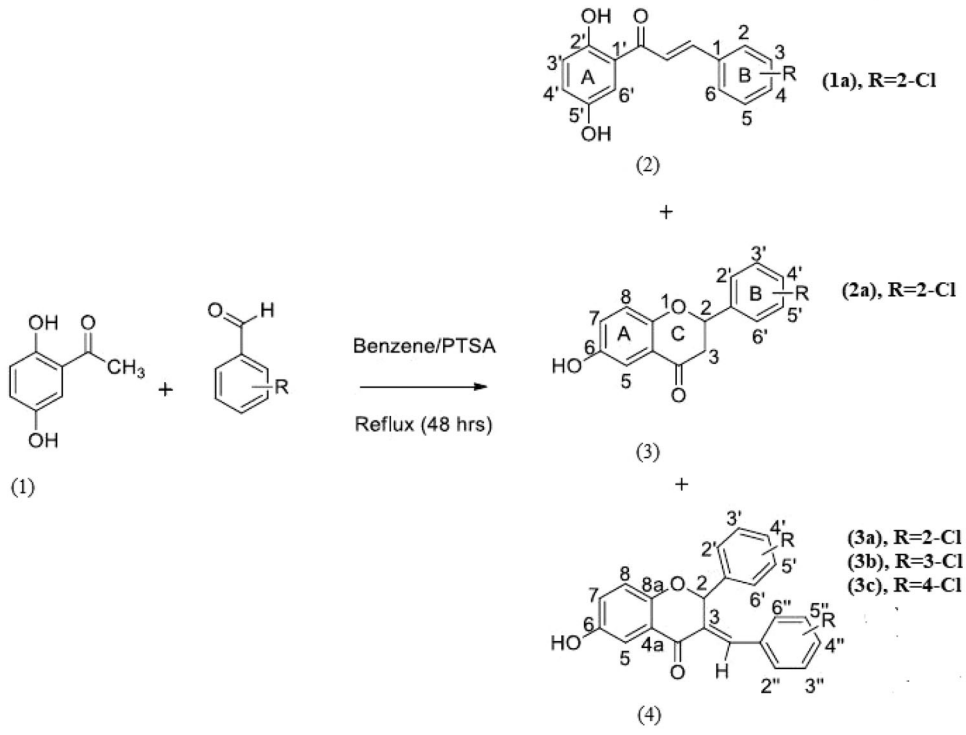

Scheme 1. Synthesis of chloro-substituted hydroxychalcones **(2)**, hydroxyflavanones **(3)** and hydroxyflavindogenides **(4).**

Table 1. Physicochemical characterization data of the synthesized compounds.

Compound	-R	Molecular formula	Molecular weight	Melting point (°C)	Yield (%)
1a	2-Cl	$C_{15}H_{11}O_3Cl$	274.6	213	18
2a	2-Cl	$C_{15}H_{11}$ O_3Cl	274.6	202	12
3a	2-Cl	$C_{22}H_{14}$ O_3Cl_2	396.2	276	17
3b	3-Cl	$C_{22}H_{14}$ O_3Cl_2	396.1	289	34
3c	4-Cl	$C_{22}H_{14}$ O_3Cl_2	396.1	292	38

and Atomic Contact Energy (ACE). Furthermore hydrogen bonding and hydrophobic interactions were also recorded in the vicinity of binding pocket using Discovery Studio 4.5 Visualizer.

Computational detail

To understand the radical scavenging procedure H-atom transfer and one-electron transfer mechanisms are frequently used (Belcastro et al., 2006; Wright et al., 2001). In the present study, we have shed light on the one-electron transfer mechanism. Recently, density functional theory (DFT) has been proved proficient method that reproduces the experimental data (Chaudhry et al., 2014a, 2014b; Irfan & Al-Sehemi, 2014). The ground state geometries were optimized by using B3LYP functional (Irfan et al., 2016, 2017) and 6-31G** basis set. Details about methodology can be found in the reference. Ionization potentials (IP) have been calculated as under (Al-Sehemi et al., 2016).

$$IP = -E_{HOMO} \quad (1)$$

$$EA = -E_{LUMO} \quad (2)$$

All calculations were performed by Spartan '14 v1.1.8' at B3LYP/6-31G** level which has been proved an efficient and reasonable approach to shed light on the structure-activity relationship and other physiochemical properties (Al-Sehemi et al., 2016, 2017).

Results and discussion

Flavonoid derivatives chalcone **(1a)**, flavanone **(2a)** and flavindogenides **(3a-3c)** were isolated from the reaction mixture of 2,5-dihydroxyacetophenone and chlorobenzaldehydes. Benzene was chosen as a best solvent among the various endeavoured solvent systems like methanol, ethanol, 2-propanol and toluene. 1H NMR, 13C NMR techniques were used to characterize the synthesized compounds. Appearance of two doublets with $J = 15.6$ corresponding α and β proton of the ethene linkage was a prominent identification for the synthesis of chalcones. Absence of these signals and appearance of signals at δ 5.75, 3.22, and 2.88 confirming the 2-H, 3Ha and 3Hb of the hetero ring signposted the formation of flavanones. The synthetic scheme of flavanones, chalcones and flavindogenides from 2,5-dihydroxyacetophenone and benzaldehydes is given in scheme 1, whereas the physiochemical data of the synthesized compounds is summarized in Table 1.

Table 2. DPPH radical scavenging activity of tested compounds.

	IC_{50} (μ M) values at different times (minutes)				
Compounds	15	30	45	60	120
Torolx	225.12 ± 15.12	216.25 ± 10.41	223.18 ± 15.01	214.83 ± 10.43	252.73 ± 17.22
Ascorbic acid	215.50 ± 10.43	221.36 ± 14.81	234.44 ± 15.71	244.46 ± 15.91	240.47 ± 15.81
1a	91.7 ± 8.34	117 ± 16.89	173 ± 46.34	134 ± 18.46	234 ± 9.57
2a	>2000	>2000	>2000	>2000	>2000
3a	>2000	>2000	>2000	>2000	>2000
3b	>2000	>2000	>2000	>2000	>2000
3c	>2000	>2000	>2000	>2000	>2000

Table 3. ABTS activity of tested compounds.

	IC_{50} (μM) at different times (minutes)					
Compounds	5	15	30	45	60	120
Torolx	32.31 ± 0.21	51.56 ± 0.32	50.38 ± 1.32	53.56 ± 1.78	31.97 ± 1.43	29.33 ± 1.27
Ascorbic acid	76.79 ± 0.89	109.46 ± 1.52	97.47 ± 4.36	64.19 ± 2.11	45.23 ± 1.92	37.91 ± 1.74
1a	15.32 ± 0.34	16.34 ± 0.45	18.30 ± 1.67	19.53 ± 2.98	18.71 ± 1.78	17.35 ± 1.67
2a	96.4 ± 12.76	83.21 ± 14.76	74.3 ± 12.89	68.2 ± 16.23	54.2 ± 10.98	43.1 ± 23.76
3a	30.42 ± 1.23	43.25 ± 2.16	48.56 ± 2.17	50.51 ± 1.32	52.60 ± 0.98	47.37 ± 1.65
3b	60.22 ± 0.76	63.50 ± 2.34	86.31 ± 3.56	102.54 ± 4.21	91.23 ± 1.45	90.78 ± 1.67
3c	82.58 ± 3.21	84.56 ± 4.51	94.51 ± 5.32	103.65 ± 3.22	120.45 ± 2.89	101.89 ± 2.99

Table 4. Iron chelating activity of tested compounds.

	IC_{50} (μM) at different times (minutes)				
Compounds	15	30	45	60	120
Torolx	0.46 ± 0.23	0.49 ± 0.25	0.53 ± 0.32	0.41 ± 0.24	0.28 ± 0.11
Ascorbic acid	3.33 ± 1.19	2.15 ± 1.13	0.33 ± 0.67	0.23 ± 0.52	0.24 ± 0.59
1a	5.05 ± 1.89	3.24 ± 2.45	3.56 ± 1.35	3.12 ± 0.76	2.78 ± 1.90
2a	6.327 ± 11.34	18.281 ± 9.45	33.36 ± 10.54	40.722 ± 12.89	39.176 ± 6.45
3a	96.807 ± 1.11	78.514 ± 1.09	368.31 ± 1.23	112.037 ± 2.45	109.43 ± 1.56
3b	223.91 ± 2.45	316.22 ± 2.76	474.41 ± 1.78	815.2 ± 1.98	856 ± 0.23
3c	615.34 ± 2.13	438.51 ± 1.34	420.23 ± 1.23	424.81 ± 0.98	501.23 ± 0.23

Table 5. $FeCl_3$ reducing power activity of tested compounds.

	IC_{50} (μM) at different times (minutes)				
Compounds	15	30	45	60	120
Torolx	13.75 ± 2.45	12.04 ± 3.07	11.24 ± 2.74	11.43 ± 1.98	10.06 ± 2.24
Ascorbic acid	14.64 ± 3.34	14.74 ± 3.29	14.02 ± 3.12	13.16 ± 3.54	12.74 ± 2.87
1a	14.12 ± 6.73	16.34 ± 3.89	17.34 ± 7.32	15.23 ± 1.90	14.34 ± 1.92
2a	35.25 ± 17.35	32.19 ± 16.23	30.25 ± 23.41	27.16 ± 2.87	25.41 ± 1.76
3a	19.87 ± 4.56	21.47 ± 4.78	23.328 ± 8.23	23.019 ± 9.34	24.766 ± 1.34
3b	22.56 ± 5.34	24.23 ± 2.67	27.4 ± 1.89	29.56 ± 8.45	30.12 ± 3.67
3c	114.4 ± 5.27	78.2 ± 1.89	74.50 ± 5.78	75.50 ± 3.87	52.61 ± 5.23

In vitro antioxidant activities

The radical scavenging activity of the tested compounds was evaluated by their interaction with DPPH free radical. The tested compounds except 1a were not good DPPH radical scavengers and showed IC_{50} values more than 2000 μM compared to standard compounds. Compound 1a showed excellent IC_{50} (91.7 ± 8.34, 117 ± 16.89, 173 ± 46.34, 134 ± 18.46, and 234 ± 9.57) at different time intervals compared with Trolox and Ascorbic acid. Increasing order was observed in the IC_{50} of tested compounds (Table 2).

All the compounds were tested for ABTS activity in time dependent and concentration dependent manner. IC_{50} values for all the compounds and standard compounds were depicted in Table 3.

All the tested compounds showed impressive IC_{50}. Especially, compound 1a showed prominent ABTS compared with standard compounds at 5, 15, 30, 45, 60 and 120 mins of incubation. IC_{50} of compound 3a was comparable to trolox and lower than ascorbic acid up to 45 mins of activity. Overall the order of activity of the tested compounds was 1a > 3a> 2a > 3b > 3c.

Table 6. Phosphomolybdenum assay for all tested compounds.

	IC_{50} (μM) at different times (minutes)		
Compounds	15	30	45
Trolox	16.25 ± 2.35	15.89 ± 2.73	15.25 ± 3.43
Ascorbic acid	21.73 ± 1.23	17.37 ± 3.61	15.82 ± 1.58
1a	24.74 ± 0.67	26.34 ± 0.99	28.31 ± 1.23
2a	67.45 ± 1.34	57.82 ± 2.56	43.21 ± 2.89
3a	11.56 ± 6.54	13.71 ± 4.32	12.80 ± 7.23
3b	13.74 ± 5.32	18.45 ± 8.54	19.70 ± 8.32
3c	20.30 ± 9.12	22.78 ± 8.43	25.81 ± 10.11

The tested compounds were examined for their reducing ability of ferric ions. The synthesized compounds reduced

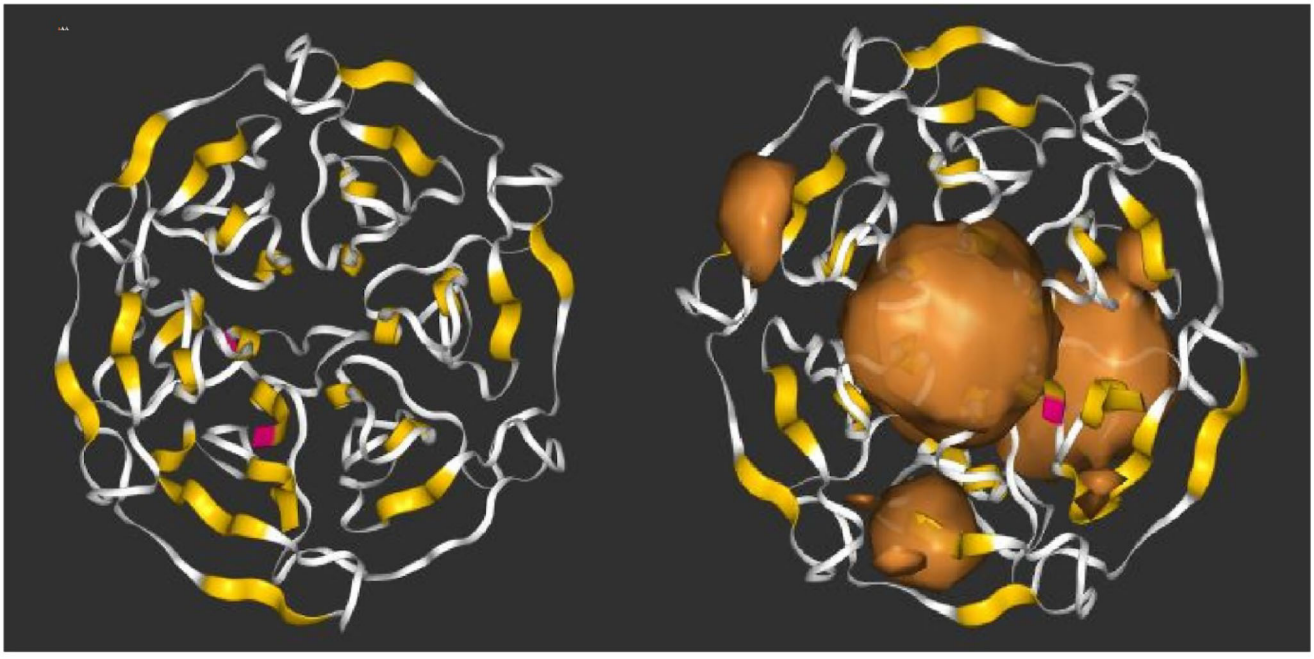

Figure 3. Three-dimensional structure and binding pocket of Keap1(PDB ID: 2FLU).

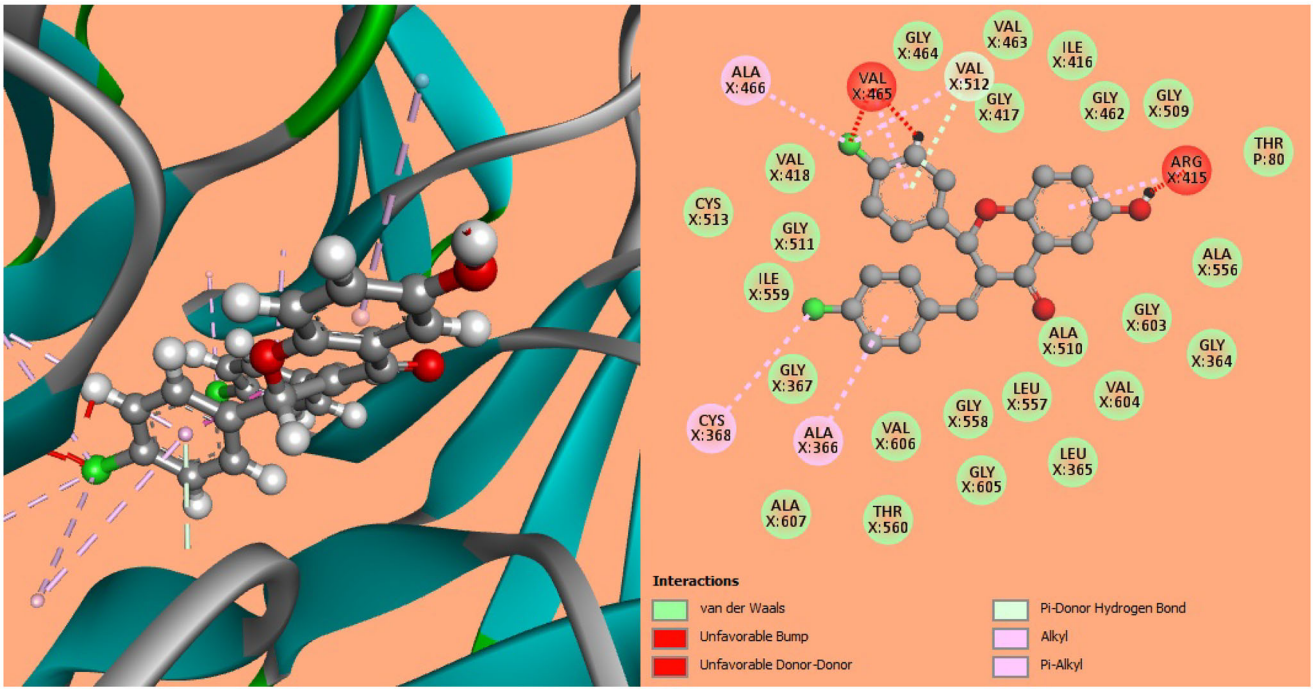

Figure 4. Three-dimensional and two-dimensional view of binding site interaction of most potent compound 3c.

ferric ions to ferrous which forms complex with o-phenanthroline. Compound 1a exhibited greater chelating power and showed the lowest IC_{50} value among all the tested compounds. The reducing power of the test compounds in terms of their IC_{50} values was calculated and depicted in Table 4. The increasing order of reducing power of tested compounds was 1a > 2a > 3a> 3b > 3c.

The tested compounds reduced potassium ferricyanide (Fe^{+3}) to potassium ferrocyanide (Fe^{+2}) which formed ferric ferrous complex on reaction with ferric chloride. The IC_{50} values of all the tested compounds corresponding to their reducing abilities were summarised in Table 5. All compounds showed impressive and comparable IC_{50} values with

Table 7. Molecular docking evaluation of tested compounds.

Compounds	Docking score	Area	ACE
Trolox	3934	425.30	−238.17
Ascorbic acid	2984	301.90	−143.24
1a	4546	480.00	−288.15
2a	4416	458.70	−284.42
3a	4760	523.00	−386.89
3b	5270	557.80	−402.47
3c	5368	622.40	−438.96

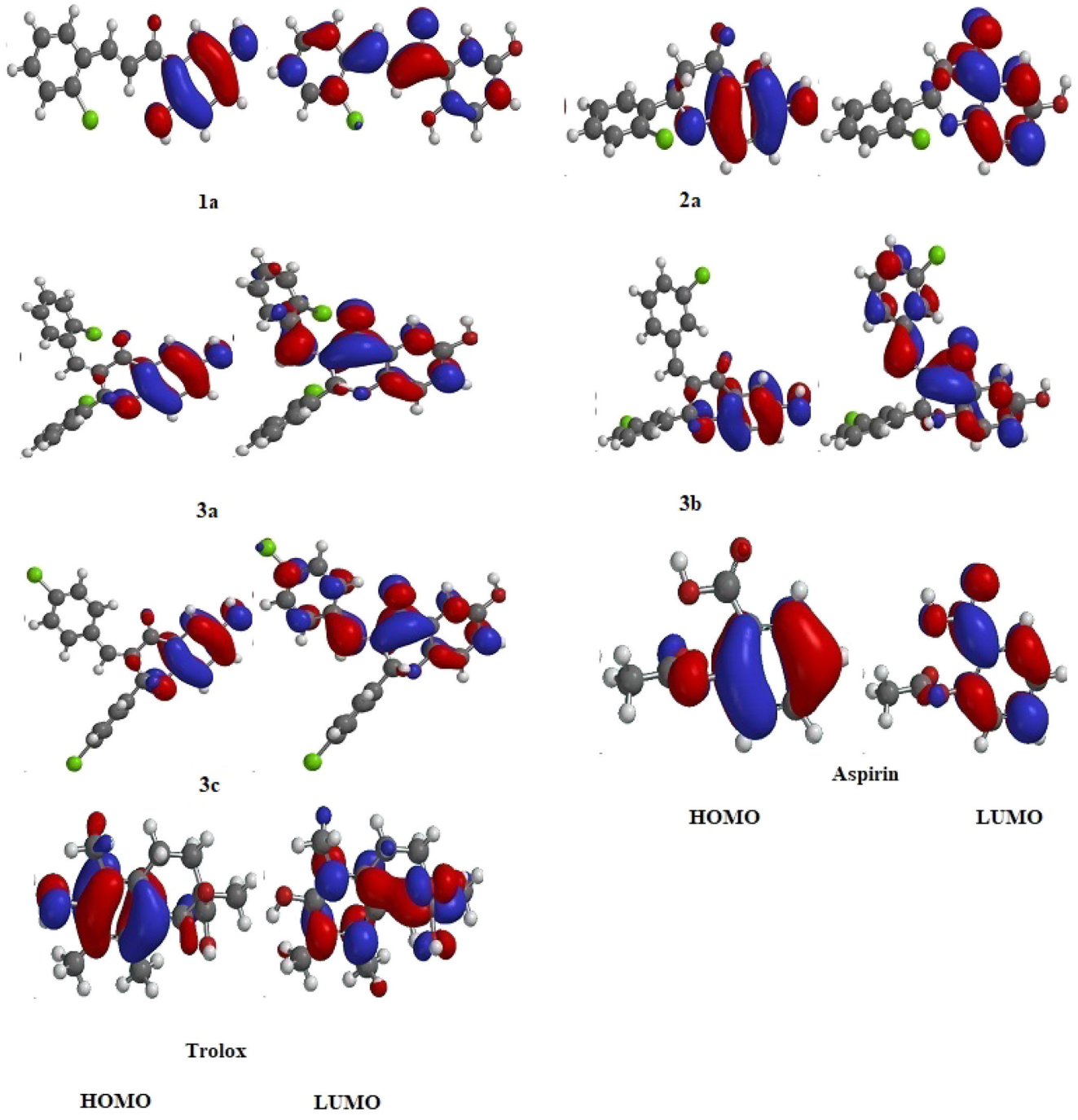

Figure 5. The distribution pattern of the HOMOs and LUMOs of chloro-substituted hydroxychalcone (1a), hydroxyflavanone (2a), hydroxyflavindogenides (3a-3c), aspirin and trolox at ground states.

Table 8. Different HOMO energies (E_{HOMO}), LUMO energies (E_{LUMO}), HOMO-LUMO gaps (E_{gap}), ionization potentials (IP) and electron affinities (EA) in eV of studied compounds obtained at B3LYP/6-31G** level of theory.

Compounds	E_{HOMO}	E_{LUMO}	E_{gap}	IP	EA
Trolox	−5.42	0.12	5.54	5.42	−0.12
Aspirin	−7.00	−1.46	5.54	7.00	1.46
1a	−5.68	−2.05	3.63	5.68	2.05
2a	−5.65	−1.98	3.67	5.65	1.98
3a	−5.76	−1.55	4.21	5.76	1.55
3b	−5.44	−1.72	3.72	5.44	1.72
3c	−5.82	−2.23	3.59	5.82	2.23

ascorbic acid and trolox. The reducing power of the tested compounds in increasing order was 1a > 3a > 2a > 3b > 3c.

Furthermore, in PM activity, Mo^{+6} reduced to Mo^{+5} by gaining electron. This reduction ability of all tested were calculated by phosphomolybdenum assay and depicted their IC_{50} values in Table 6. All compounds showed excellent reduction ability in comparison with each other and reference compounds. The order of strength of tested compounds to reduce the molybdenum was 3a > 3b > 3c > 1a > 2a.

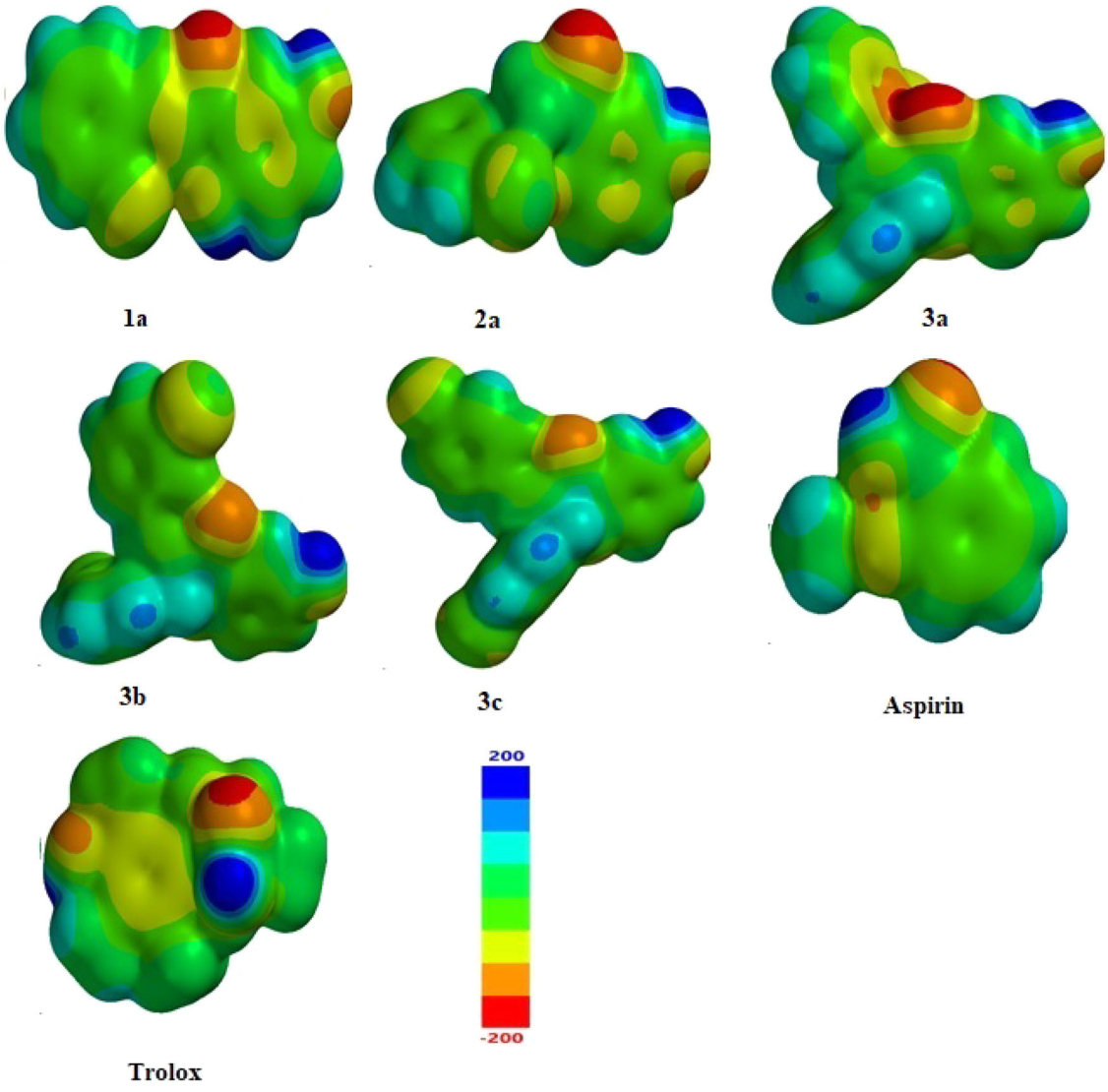

Figure 6. The molecular electrostatic potential surfaces of chloro-substituted hydroxychalcone (1a), hydroxyflavanone (2a), hydroxyflavindogenides (3a-3c), aspirin and trolox.

Table 9. Different QSAR descriptors of studied compounds obtained at B3LYP/6-31G** level of theory.

Compounds	μD (Debye)	Area (A^2)	Volume (A^3)	Log *P*	HBD	HBA	Pol.	PSA (A^2)	SE (kJ/mol)
1a	2.67	271.46	254.63	0.21	2	3	61.17	50.21	–50.16
2a	3.17	335.37	349.94	0.09	1	3	68.89	38.87	–46.47
3a	2.63	261.84	261.64	–0.52	1	3	60.55	41.15	–38.57
3b	2.77	403.52	395.08	–0.80	1	5	72.54	48.73	–49.20
3c	1.16	287.77	268.48	0.88	2	3	62.31	50.28	–53.54

μD = dipole moment; HBD = hydrogen bond donor; HBA = hydrogen bond acceptor; PSA = polar surface area; SE = solvation energy; Pol. = Polarizability).

In silico studies

All the synthesized compounds were docked with the binding site of the Keap1, a potent inhibitor of Nrf2. Figures 3 and 4 and supporting material S2–S7 depicted the binding pockets of Keap1 protein and their binding interaction with tested compounds, while their docking scores, area and ACE values were presented in Table 7. Overall all, synthesized compounds exhibited better docking score, greater area and lower ACE values compared to ascorbic acid and trolox. Comparatively, flavindogenides showed high docking score among the synthesized flavonoid derivatives particularly compound 3c, substituted at position C-4 of the flavindogenide exhibited the highest docking score 5368, area 622 and lowest ACE –438.96 when compared with other flavindogenides and reference compounds. High docking score and lower ACE values supports the affinity of ligand with receptor protein (Schneidman-Duhovny et al., 2005). Protein-ligand interactions encountering van der Waal's, hydrogen bonds, carbon hydrogen bonds and unfavourable bumps were visualized with DS. Amino acids of the Kelch domain of Keap1 make interactions with the Nrf2 (Li et al., 2004; Lo et al., 2006). C-4 substituted flavonoid derivative (3c) seems to make interactions with the target protein in the Kelch domain. It makes interactions with residues Ala366,

Cys368, Val465, Ala466, Val512 of 2FLU (Figure 4). Disruption of Nrf2-Keap1 interaction favours the activation of Nrf2 and suppression of oxidative stress, inflammation and related diseases (Li et al., 2008).

Electronic properties

The distribution pattern of the frontier molecular orbitals (FMOs), e.g. highest occupied molecular orbitals (HOMOs) and lowest unoccupied molecular orbitals (LUMOs) of all compounds have been illustrated in Figure 5. In all the studied compounds, the intra-molecular charge transfer (ICT) has been observed from HOMO to LUMO. In Table 8, we have tabulated the HOMO energies (E_{HOMO}), LUMO energies (E_{LUMO}), HOMO to LUMO energy gaps (E_{gap}), IP and EA at the B3LYP/6-31G** level of theory. The E_{HOMO} levels of indigenously synthesized and studied compounds are lower than the trolox while higher than aspirin. The E_{LUMO} levels of studied compounds are lower than the trolox while higher than aspirin. The E_{gap} of all the compounds is smaller than the trolox and aspirin. Additionally, with respect to charge transfer ability of the compounds, it is expected that the higher EA of all the compounds than the referenced compounds (aspirin and trolox) showed that prior compounds might lead to better electron transport ability. The scavenging of free radical can be evaluated by single electron donation. IP is an important descriptor by which the range of electron transfer can be assessed. By removing electron from HOMO, one-electron transfer radical cation can be gained. It can be seen from Table 8 that the smaller IP values of studied compounds as compared to the aspirin enlightening that in aforementioned compounds electron transfer mechanism might be more promising for the scavenging of free radicals than referenced compounds.

Molecular electrostatic potential

The three-dimensional surface maps of the molecular electrostatic potential (MEP) are best tool to know the molecular interactions as well as the relative reactivity sites for the nucleophilic and electrophilic attack. In Figure 6, we have illustrated the MEP surface maps of all the studied compounds along with reference compounds to understand the positive and negative electrostatic potential (ESP) regions. Furthermore, three different colours including red, blue and green colours represent the negative, positive and zero potential regions. It is anticipated that the electrophilic and nucleophilic attack would be favourable on the negative and positive ESP, respectively.

QSAR study

In Table 9, we have tabulated different QSAR descriptors e.g. μD = dipole moment, area, volume, partition coefficient (Log*P*), hydrogen bond donor (HBD), hydrogen bond acceptor (HBA), polar surface area (PSA), solvation energy and polarizability of studied compounds. Previously, it has been shown that PSA should not exceed 120 A^2 for the orally active drug which are transported by transcellular route (Kelder et al., 1999; van de Waterbeemd et al., 1998) and $<100\ A^2$ for brain penetration (van de Waterbeemd et al., 1998) or $<60–70\ A^2$ (Kelder et al., 1999). The PSA of all the studied compounds is less than 60 A^2.

Moreover, the PSA of all the studied compounds is also smaller than the referenced compound aspirin. On other, lipophilicity of the most of the studied compounds is smaller than the aspirin and trolox. From the previous studies, it is widely accepted that the compounds having very high/low log*P* values do not have good bio-availability as they cannot cross hydrophilic and lipophilic barricades, respectively. Compound having intermediate log *P* values have more probability to attain at the receptor site.

A negative value for log*P* means the compound has a higher affinity for the aqueous phase (it is more hydrophilic); when log*P* = 0 the compound is equally partitioned between the lipid and aqueous phases; a positive value for log*P* denotes a higher concentration in the lipid phase (i.e. the compound is more lipophilic). It is expected that 3a and 3b have negative log*P* values revealing that these compounds might be hydrophilic. While all other compounds have positive values illuminating that these compounds might be more lipophilic.

Conclusion

Acid catalysed condensation reaction of various chlorobenzaldehydes with 2,5-dihydroxyacetophenone gives chalcones, flavanones and flavindogenides. All the synthesized compounds exhibited good antioxidant potential. QASR studies and molecular docking results revealed that aforesaid compounds manifested comprehensive intra-molecular charge transfer from the HOMOs to the LUMOs with smaller IP and E_{gap} values, and high docking score for Nrf2 activation compared to referenced compounds. Based on these evidences, tested compounds especially 3c might be used to suppress the inflammation by changing the conformation of Keap1 and activating Nrf2-ARE-Keap1 pathway.

Disclosure statement

The authors declare that they have no conflict of interest.

Funding

This work is supported by the Higher Education Commission (HEC), Pakistan and the School of Chemistry, University of the Punjab, Lahore, Pakistan. Ahmad Irfan is thankful to the Deanship of Scientific Research at King Khalid University, Saudi Arabia through a research groups program under grant number R.G.P. 1/12/42.

ORCID

Ahmad Irfan http://orcid.org/0000-0001-6941-6934
Muhammad Asim Raza Basra http://orcid.org/0000-0002-4242-0025

References

Abotaleb, M., Samuel, S. M., Varghese, E., Varghese, S., Kubatka, P., Liskova, A., & Büsselberg, D. (2018). Flavonoids in cancer and apoptosis. *Cancers*, *11*(1), 28. https://doi.org/10.3390/cancers11010028

Al-Sehemi, A. G., Irfan, A., Alfaifi, M., Fouda, A. M., El-Gogary, T. M. M., & Ibrahim, D. A. (2017). Computational study and in vitro evaluation of the anti-proliferative activity of novel naproxen derivatives. *Journal of King Saud University - Science*, *29*(3), 311–319. https://doi.org/10.1016/j.jksus.2017.01.003

Al-Sehemi, A. G., Irfan, A., Aljubiri, S. M., & Shaker, K. H. (2016). Density functional theory investigations of radical scavenging activity of 3′-methyl-quercetin. *Journal of Saudi Chemical Society*, *20*, S21–S28. https://doi.org/10.1016/j.jscs.2012.08.004

Al-Sehemi, A. G., Irfan, A., Alrumman, S. A., & Hesham, A. (2016). Antibacterial activities, DFT and QSAR studies of quinazolinone compounds. *Bulletin of the Chemical Society of Ethiopia*, *30*(2), 307–316. https://doi.org/10.4314/bcse.v30i2.15

Amic, D., Davidovic-Amic, D., Beslo, D., Rastija, V., Lucic, B., & Trinajstic, N. (2007). SAR and QSAR of the antioxidant activity of flavonoids. *Current Medicinal Chemistry*, *14*(7), 827–845. https://doi.org/10.2174/092986707780090954

Amin, G., & Shah, N. (2003). 5-Dihydroxyacetophenone: Acetophenone, 2, 5-dihydroxy-quinacetophenone. *Organic Syntheses*, *2*, 42–42. https://doi.org/10.1002/0471264180.os028.17

Ashraf, J., Mughal, E. U., Alsantali, R. I., Obaid, R. J., Sadiq, A., Naeem, N., Ali, A., Massadaq, A., Javed, Q., Javid, A., Sumrra, S. H., Zafar, M. N., & Ahmed, S. A. (2021). Structure-based designing and synthesis of 2-phenylchromone derivatives as potent tyrosinase inhibitors: In vitro and in silico studies. *Bioorganic & Medicinal Chemistry*, *35*, 116057. https://doi.org/10.1016/j.bmc.2021.116057

Ashraf, J., Mughal, E. U., Sadiq, A., Bibi, M., Naeem, N., Ali, A., Massadaq, A., Fatima, N., Javid, A., & Zafar, M. N. (2020). Exploring 3-hydroxyflavone scaffolds as mushroom tyrosinase inhibitors: Synthesis, X-ray crystallography, antimicrobial, fluorescence behaviour, structure-activity relationship and molecular modelling studies. *Journal of Biomolecular Structure and Dynamics*, 1–16. https://doi.org/10.1080/07391102.2020.1805364

Ashraf, J., Mughal, E. U., Sadiq, A., Naeem, N., Muhammad, S. A., Qousain, T., Zafar, M. N., Khan, B. A., & Anees, M. (2020). Design and synthesis of new flavonols as dual α-amylase and α-glucosidase inhibitors: Structure-activity relationship, drug-likeness, in vitro and in silico studies. *Journal of Molecular Structure*, *1218*, 128458. https://doi.org/10.1016/j.molstruc.2020.128458

Athar, M., Lone, M. Y., Khedkar, V. M., & Jha, P. C. (2016). Pharmacophore model prediction, 3D-QSAR and molecular docking studies on vinyl sulfones targeting Nrf2-mediated gene transcription intended for anti-Parkinson drug design. Journal of Biomolecular Structure and Dynamics, *34*(6), 1282–1297. https://doi.org/10.1080/07391102.2015.1077343

Atwood, J. J., & Buck, W. R. (2020). Recent literature on bryophytes. *The Bryologist*, *123*(3), 547–583. https://doi.org/10.1639/0007-2745-123.3.547

Belcastro, M., Marino, T., Russo, N., & Toscano, M. (2006). Structural and electronic characterization of antioxidants from marine organisms. *Theoretical Chemistry Accounts*, *115*(5), 361–369. https://doi.org/10.1007/s00214-006-0077-5

Bresciani, A., Missineo, A., Gallo, M., Cerretani, M., Fezzardi, P., Tomei, L., Cicero, D. O., Altamura, S., Santoprete, A., Ingenito, R., Bianchi, E., Pacifici, R., Dominguez, C., Munoz-Sanjuan, I., Harper, S., Toledo-Sherman, L., & Park, L. C. (2017). Nuclear factor (erythroid-derived 2)-like 2 (NRF2) drug discovery: Biochemical toolbox to develop NRF2 activators by reversible binding of Kelch-like ECH-associated protein 1 (KEAP1). *Archives of Biochemistry and Biophysics*, *631*, 31–41. https://doi.org/10.1016/j.abb.2017.08.003

Chaudhry, A. R., Ahmed, R., Irfan, A., Muhammad, S., Shaari, A., & Al-Sehemi, A. G. (2014a). Effect of heteroatoms substitution on electronic, photophysical and charge transfer properties of naphtha [2, 1-b: 6, 5-b′] difuran analogues by density functional theory. *Computational and Theoretical Chemistry*, *1045*, 123–134. https://doi.org/10.1016/j.comptc.2014.06.028

Chaudhry, A. R., Ahmed, R., Irfan, A., Shaari, A., Maarof, H., & Al-Sehemi, A. G. (2014b). First principles investigations of electronic, photoluminescence and charge transfer properties of the naphtho [2, 1-b: 6, 5-b′] difuran and its derivatives for OFET. *Sains Malaysiana*, *43*(6), 867–875. https://doi.org/10.1016/j.comptc.2014.06.028

Górniak, I., Bartoszewski, R., & Króliczewski, J. (2019). Comprehensive review of antimicrobial activities of plant flavonoids. *Phytochemistry Reviews*, *18*(1), 241–272. https://doi.org/10.1007/s11101-018-9591-z

Halliwell, B., Aeschbach, R., Löliger, J., & Aruoma, O. (1995). The characterization of antioxidants. *Food and Chemical Toxicology : An International Journal Published for the British Industrial Biological Research Association*, *33*(7), 601–617. https://doi.org/10.1016/0278-6915(95)00024-V

Heim, K. E., Tagliaferro, A. R., & Bobilya, D. J. (2002). Flavonoid antioxidants: Chemistry, metabolism and structure-activity relationships. *The Journal of Nutritional Biochemistry*, *13*(10), 572–584. https:// https://doi.org/10.1016/S0955-2863(02)00208-5

Irfan, A., & Al-Sehemi, A. G. (2014). DFT study of the electronic and charge transfer properties of perfluoroarene–thiophene oligomers. *Journal of Saudi Chemical Society*, *18*(5), 574–580. https://doi.org/10.1016/j.jscs.2011.11.006

Irfan, A., Al-Sehemi, A. G., Chaudhry, A. R., Muhammad, S., & Asiri, A. M. (2016). The structural, electro-optical, charge transport and nonlinear optical properties of 2-[(3, 5-dimethyl-1-phenyl-1H-pyrazol-4-yl) methylidene] indan-1, 3-dione. *Optik*, *127*(21), 10148–10157. https://doi.org/10.1016/j.ijleo.2016.08.007

Irfan, A., Kalam, A., Chaudhry, A. R., Al-Sehemi, A. G., & Muhammad, S. (2017). Electro-optical, nonlinear and charge transfer properties of naphthalene based compounds: A dual approach study. *Optik*, *132*, 101–110. https://doi.org/10.1016/j.ijleo.2016.12.023

Jiménez, J., Doerr, S., Martínez-Rosell, G., Rose, A. S., & De Fabritiis, G. (2017). DeepSite: Protein-binding site predictor using 3D-convolutional neural networks. *Bioinformatics (Oxford, England)*, *33*(19), 3036–3042. https://doi.org/10.1093/bioinformatics/btx350

Karak, P. (2019). Biological activities of flavonoids: An overview. *International Journal of Pharmaceutical Sciences and Research*, *10*(4), 1567–1574. https://doi.org/10.13040/IJPSR.0975-8232.10(4).1567-74

Kelder, J., Grootenhuis, P. D., Bayada, D. M., Delbressine, L. P., & Ploemen, J.-P. (1999). Polar molecular surface as a dominating determinant for oral absorption and brain penetration of drugs. *Pharmaceutical Research*, *16*(10), 1514–1519. https://doi.org/10.1023/A:1015040217741

Li, L., Luo, W., Qian, Y., Zhu, W., Qian, J., Li, J., Jin, Y., Xu, X., & Liang, G. (2019). Luteolin protects against diabetic cardiomyopathy by inhibiting NF-κB-mediated inflammation and activating the Nrf2-mediated antioxidant responses. *Phytomedicine : International Journal of Phytotherapy and Phytopharmacology*, *59*, 152774 https://doi.org/10.1016/j.phymed.2018.11.034

Li, W., Khor, T. O., Xu, C., Shen, G., Jeong, W.-S., Yu, S., & Kong, A.-N. (2008). Activation of Nrf2-antioxidant signaling attenuates NFkappaB-inflammatory response and elicits apoptosis. Biochemical Pharmacology, *76*(11), 1485–1489. https://doi.org/10.1016/j.bcp.2008.07.017

Li, X., Zhang, D., Hannink, M., & Beamer, L. J. (2004). Crystal structure of the Kelch domain of human Keap1. *The Journal of Biological Chemistry*, *279*(52), 54750–54758. https://doi.org/10.1074/jbc.M410073200

Li, Y.-R., Li, G.-H., Zhou, M.-X., Xiang, L., Ren, D.-M., Lou, H.-X., Wang, X.-N., & Shen, T. (2018). Discovery of natural flavonoids as activators of Nrf2-mediated defense system: Structure-activity relationship and inhibition of intracellular oxidative insults. *Bioorganic & Medicinal Chemistry*, *26*(18), 5140–5150. https://doi.org/10.1016/j.bmc.2018.09.010

Lo, S. C., Li, X., Henzl, M. T., Beamer, L. J., & Hannink, M. (2006). Structure of the Keap1:Nrf2 interface provides mechanistic insight into Nrf2 signaling. *The EMBO Journal*, *25*(15), 3605–3617. https://doi.org/10.1038/sj.emboj.7601243

Maleki, S. J., Crespo, J. F., & Cabanillas, B. (2019). Anti-inflammatory effects of flavonoids. *Food Chemistry*, *299*, 125124. https://doi.org/10.1016/j.foodchem.2019.125124

Mao, X., Gu, C., Chen, D., Yu, B., & He, J. (2017). Oxidative stress-induced diseases and tea polyphenols. *Oncotarget*, *8*(46), 81649–81661. https://doi.org/10.18632/oncotarget.20887

Mughal, E. U., Sadiq, A., Ayub, M., Naeem, N., Javid, A., Sumrra, S. H., Zafar, M. N., Khan, B. A., Malik, F. P., & Ahmed, I. (2020). Exploring 3-Benzyloxyflavones as new lead cholinesterase inhibitors: Synthesis, structure–activity relationship and molecular modelling simulations. *Journal of Biomolecular Structure and Dynamics*, 1–14. https://doi.org/10.1080/07391102.2020.1803136

Pietta, P.-G. (2000). Flavonoids as antioxidants. Journal of Natural Products, *63*(7), 1035–1042. https://doi.org/10.1021/np9904509

Sarian, M. N., Ahmed, Q. U., Mat So'ad, S. Z., Alhassan, A. M., Murugesu, S., Perumal, V., Syed Mohamad, S. N. A., Khatib, A., & Latip, J. (2017). Antioxidant and antidiabetic effects of flavonoids: A structure-activity relationship based study. *BioMed Research International*, *2017*, 8386065. https://doi.org/10.1155/2017/8386065

Schneidman-Duhovny, D., Inbar, Y., Nussinov, R., & Wolfson, H. J. (2005). PatchDock and SymmDock: Servers for rigid and symmetric docking. *Nucleic Acids Research*, *33*(Web Server issue), W363–W367. https://doi.org/10.1093/nar/gki481

Singh, D., Verma, S., & Prabha, R. (2018). Investigations on antioxidant potential of phenolic acids and flavonoids: The common phytochemical ingredients in plants. *Journal of Plant Biochemistry and Physiology*, *6*, 1000219. https://doi.org/10.4172/2329-9029.1000219

Su, X., Huang, Q., Chen, J., Wang, M., Pan, H., Wang, R., Zhou, H., Zhou, Z., Liu, J., Yang, F., Li, T., & Liu, L. (2016). Calycosin suppresses expression of pro-inflammatory cytokines via the activation of p62/Nrf2-linked heme oxygenase 1 in rheumatoid arthritis synovial fibroblasts. *Pharmacological Research*, *113*(Pt A), 695–704. https://doi.org/10.3390/molecules24173116

Sun, Y., Yang, T., K Leak, R., Chen, J., & Zhang, F. (2017). Preventive and protective roles of dietary Nrf2 activators against central nervous system diseases. *CNS & Neurological Disorders Drug Targets*, *16*(3), 326–338. https://doi.org/10.2174/1871527316666170102120211

Tajammal, A., Batool, M., Ramzan, A., Samra, M. M., Mahnoor, I., Verpoort, F., Irfan, A., Al-Sehemi, A. G., Munawar, M. A., & Basra, M. A. R. (2017). Synthesis, antihyperglycemic activity and computational studies of antioxidant chalcones and flavanones derived from 2, 5 dihydroxyacetophenone. *Journal of Molecular Structure*, *1148*, 512–520. https://doi.org/10.1016/j.molstruc.2017.07.042

Tran, P.-L., Tran, P. T., Tran, H. N. K., Lee, S., Kim, O., Min, B.-S., & Lee, J.-H. (2018). A prenylated flavonoid, 10-oxomornigrol F, exhibits anti-inflammatory effects by activating the Nrf2/heme oxygenase-1 pathway in macrophage cells. *International Immunopharmacology*, *55*, 165–173. https://doi.org/10.1016/j.intimp.2017.12.015

van de Waterbeemd, H., Camenisch, G., Folkers, G., Chretien, J. R., & Raevsky, O. A. (1998). Estimation of blood-brain barrier crossing of drugs using molecular size and shape, and H-bonding descriptors. *Journal of Drug Targeting*, *6*(2), 151–165. https://doi.org/10.3109/10611869808997889

Wang, G., Xie, X., Yuan, l., Qiu, J., Duan, W., Xu, B., & Chen, X. (2020). Resveratrol ameliorates rheumatoid arthritis via activation of SIRT1-Nrf2 signaling pathway . *BioFactors (Oxford, England)*, *46*(3), 441–453. https://doi.org/10.1002/biof.1599

Wright, J. S., Johnson, E. R., & DiLabio, G. A. (2001). Predicting the activity of phenolic antioxidants: Theoretical method, analysis of substituent effects, and application to major families of antioxidants. *Journal of the American Chemical Society*, *123*(6), 1173–1183. https://doi.org/10.1021/ja002455u

Wu, W.-J., Jia, W.-W., Liu, X.-H., Pan, L.-L., Zhang, Q.-Y., Yang, D., Shen, X.-Y., Liu, L., & Zhu, Y. Z. (2016). S-propargyl-cysteine attenuates inflammatory response in rheumatoid arthritis by modulating the Nrf2-ARE signaling pathway. *Redox Biology*, *10*, 157–167. https://doi.org/10.1016/j.redox.2016.08.011

Yang, J., Guo, J., & Yuan, J. (2008). In vitro antioxidant properties of rutin. *LWT - Food Science and Technology*, *41*(6), 1060–1066. https://doi.org/10.1016/j.lwt.2007.06.010

Young, I., & Woodside, J. (2001). Antioxidants in health and disease. *Journal of Clinical Pathology*, *54*(3), 176–186. https://doi.org/10.1136/jcp.54.3.176

Zhai, K.-F., Duan, H., Khan, G. J., Xu, H., Han, F.-K., Cao, W.-G., Gao, G.-Z., Shan, L.-L., & Wei, Z.-J. (2018). Salicin from *Alangium chinense* ameliorates rheumatoid arthritis by modulating the Nrf2-HO-1-ROS pathways. *Journal of Agricultural and Food Chemistry*, *66*(24), 6073–6082. https://doi.org/10.1021/acs.jafc.8b02241

Zhang, L., Zhang, W., Zheng, B., & Tian, N. (2019). Sinomenine attenuates traumatic spinal cord injury by suppressing oxidative stress and inflammation via Nrf2 pathway. *Neurochemical Research*, *44*(4), 763–775. https://doi.org/10.1007/s11064-018-02706-z